



## Research paper

## A 30 kDa polyethylene glycol-enfuvirtide complex enhances the exposure of enfuvirtide in lymphatic viral reservoirs in rats



Lisa M. Kaminskas<sup>a,\*</sup>, Charlotte C. Williams<sup>b</sup>, Nathania J. Leong<sup>c</sup>, Linda J. Chan<sup>c</sup>, Neville J. Butcher<sup>a</sup>, Orlagh M. Feeney<sup>c</sup>, Christopher J.H. Porter<sup>c</sup>, David Tyssen<sup>d,e,f,g</sup>, Gilda Tachedjian<sup>d,e,f,g</sup>, David B. Ascher<sup>h</sup>

<sup>a</sup> School of Biomedical Sciences, University of Queensland, Brisbane, St Lucia, QLD 4072, Australia

<sup>b</sup> CSIRO Materials Science and Engineering, 343 Royal Parade, Parkville, Victoria 3052, Australia

<sup>c</sup> Drug Delivery, Disposition and Dynamics, Monash Institute of Pharmaceutical Sciences, Monash University, 381 Royal Parade, Parkville, Victoria 3052, Australia

<sup>d</sup> Burnet Institute, 89 Commercial Rd, Melbourne, Victoria 3004, Australia

<sup>e</sup> Department of Microbiology, Monash University, Clayton, Victoria 3168, Australia

<sup>f</sup> Department of Microbiology and Immunology, University of Melbourne, at the Peter Doherty Institute for Infection and Immunity, Melbourne, Victoria 3000, Australia

<sup>g</sup> School of Science, College of Science, Engineering and Health, RMIT University, Melbourne, Victoria 3000, Australia

<sup>h</sup> Department of Biochemistry and Molecular Biology, Bio21 Institute, University of Melbourne, 30 Flemington Road, Parkville 3052, Australia

## ARTICLE INFO

**Keywords:**  
PEGylation  
Enfuvirtide  
Lymphatic  
Anti-viral  
Pharmacokinetics

## ABSTRACT

HIV therapy with anti-retroviral drugs is limited by the poor exposure of viral reservoirs, such as lymphoid tissue, to these small molecule drugs. We therefore investigated the effect of PEGylation on the anti-retroviral activity and subcutaneous lymphatic pharmacokinetics of the peptide-based fusion inhibitor enfuvirtide in thoracic lymph duct cannulated rats. Both the peptide and the PEG were quantified in plasma and lymph via ELISA. Conjugation to a single 5 kDa linear PEG decreased anti-HIV activity three-fold compared to enfuvirtide. Whilst plasma and lymphatic exposure to peptide mass was moderately increased, the loss of anti-viral activity led to an overall decrease in exposure to enfuvirtide activity. A 20 kDa 4-arm branched PEG conjugated with an average of two enfuvirtide peptides decreased peptide activity by six-fold. Plasma and lymph exposure to enfuvirtide, however, increased significantly such that anti-viral activity was increased two- and six-fold respectively. The results suggest that a multi-enfuvirtide-PEG complex may optimally enhance the anti-retroviral activity of the peptide in plasma and lymph.

## 1. Introduction

Despite significant worldwide efforts to develop an effective HIV vaccine, reliable immunization to prevent viral transmission remains a challenge and educational approaches to prevent infection have limited effectiveness [1]. The current standard of HIV disease management, aside from screening, education and risk management, is therefore life-long combination anti-retroviral therapy to suppress progression of the disease. To this end, over 30 anti-retroviral drugs are used in the treatment of HIV and are highly effective at reducing viral loads in plasma to below the detection limit for standard clinical assays [2]. However, these small molecule anti-retroviral drugs are ineffective at eradicating HIV virus from viral ‘reservoirs’ in resting CD4+ T and other cells that feed eventual viral rebound in plasma [3,4]. Lymphoid

tissue in particular, which is rich in CD4+ cells, is one of the major reservoirs and sites of HIV pathogenesis [5]. Specifically, HIV viral load in lymph nodes is 2–7 fold higher than in plasma, both in untreated subjects and those undergoing multiple drug therapy [5,6]. The underlying cause of high HIV viral loads in lymphatic tissue compared to plasma is a combination of high levels of target CD4+ cells as well as the typically limited exposure of lymph fluid to small molecule anti-retroviral medications [5,6]. The first step to eradicating HIV in infected individuals therefore lies in improving the exposure of these viral reservoirs to existing, and otherwise highly effective, anti-retroviral drugs.

Lymphatic exposure of small molecule drugs, for instance, can be enhanced by increasing lipophilicity via conjugation to lipid-based drug carriers, or increasing the apparent size of the drugs through

**Abbreviations:** Enf, Enfuvirtide; Cys-Enf, N-terminal cysteine-modified enfuvirtide; SEC-MALS, size exclusion chromatography-multiangle light scattering

\* Corresponding author at: School of Biomedical Sciences, University of Queensland, St Lucia, QLD 4072, Australia.

E-mail address: [l.kaminskas@uq.edu.au](mailto:l.kaminskas@uq.edu.au) (L.M. Kaminskas).

<https://doi.org/10.1016/j.ejpb.2019.03.008>

Received 4 July 2018; Received in revised form 3 March 2019; Accepted 5 March 2019

Available online 06 March 2019

0939-6411/ © 2019 Elsevier B.V. All rights reserved.

conjugation to large polymeric carriers or incorporation into drug delivery systems that can target the lymph after interstitial administration [7]. The major limitation of these approaches, however, is the ultimate need to efficiently liberate drug in plasma and lymphoid tissue, and at an efficient rate to maintain effective and maximal drug concentrations and prolonged exposure. This presents a major challenge for pharmaceutical companies and drug delivery scientists.

Enfuvirtide (Fuzeon, T-20), however, is a 4.5 kDa peptide-based anti-retroviral drug and the first marketed HIV fusion inhibitor. Despite its approximately 10-fold higher molecular weight compared to small molecule anti-retroviral drugs, it is still smaller than the threshold for effective lymphatic targeting (approx. 16–20 kDa) [8–10]. Further, it is rapidly cleared in vivo as a result of proteolytic cleavage, resulting in the need for twice daily injections of large amounts of expensive peptide (90 mg, approx. \$25G per year in the US). The limited solubility of enfuvirtide also leads to the requirement to formulate the peptide with an alkaline (pH 9) solution that causes considerable injection site pain [11].

The major advantage that enfuvirtide has as a peptide drug, is conjugation to a high molecular weight water soluble polymer can improve water solubility (avoiding the need for highly alkaline injection solutions), retention of anti-retroviral activity without the requirement for polymer release and provide for increased molecular weight and ‘stealth’ properties leading to longer plasma exposure and improved lymphatic targeting. To that end, we have previously shown that minimal (20–50% w/w) loading of protein-based therapeutics to polyethylene glycol (PEG) can significantly improve lymphatic exposure by up to an order of magnitude when compared to the unmodified protein [12–14]. The use of lower PEG loading, in particular, optimally enhances plasma and lymph exposure to protein ‘activity’ by reducing in vivo proteolysis and distribution volume, and increasing molecular mass and lymphatic targeting with limited loss of protein activity as a result of the stealth effects imparted by the PEG [14]. It is not known however, what impact PEGylation has on the activity and lymphatic pharmacokinetics of peptide-based drugs.

We therefore examined the impact of PEGylation on the anti-retroviral activity and subcutaneous lymphatic pharmacokinetics of enfuvirtide in thoracic lymph duct cannulated rats. Our central hypothesis was that relatively minimal PEGylation (or up to 50% w/w PEG) can significantly enhance plasma and lymph exposure to enfuvirtide and retain good anti-viral activity of the construct. Final construct molecular weights at or above the threshold for efficient lymphatic targeting (16–20 kDa) using, for example, conjugation to a single high molecular weight PEG, would optimally improve lymphatic access, but anti-viral activity would be significantly reduced using this approach. Working on this hypothesis, we prepared two PEGylated forms of enfuvirtide: (1) enfuvirtide conjugated to a single linear 5 kDa PEG (final MW ~ 10 kDa, 50% w/w PEG loading), and (2) enfuvirtide nominally conjugated to 3 arms of a 4-arm branched 20 kDa PEG (1-arm methoxy-PEG, 3-arm maleimide-enfuvirtide PEG, final expected MW ~ 35 kDa, approx. 57% w/w PEG loading) (Fig. 1). The rationale behind synthesising the latter construct was that it was expected to retain similar (though slightly greater) PEG loading to the smaller 5 kDa PEG-Enfuvirtide construct, and therefore presumably retain similar anti-viral activity, but would more efficiently target the lymph.

## 2. Materials and methods

### 2.1. Materials

N-terminal cysteine-modified enfuvirtide (Cys-Enf) (Ac-CYTSLIHSLEESQNQQEKNEQELLELDKWSLWNWF-NH<sub>2</sub>) > 80% purity was purchased from Pura Chemicals (Vic, Australia). Linear (5 kDa) methoxy PEG maleimide was purchased from JenKem Tech (Beijing, China) and 4-arm branched (approx. 20 kDa; 1-arm methoxy, 3-arm maleimide) PEG was obtained from Nanocs Inc (NY, USA).

Clinically available enfuvirtide (Fuzeon) was purchased from Roche (NSW, Australia). Precast NuPaGE Novex 4–12% acrylamide gels were purchased from Life Technologies (VIC, Australia). Millipore Amicon Ultra-15 centrifugal filters (3 or 10 kDa MW cutoff) were from Merck (NSW, Australia). Polyethylene and polyvinyl cannulae (0.58 × 0.96 mm internal and outer diameter respectively) were from Microtube Extrusions (NSW, Australia). Anti-enfuvirtide antibodies were custom prepared by the Monash Antibody Technologies facility (Vic, Australia). Details of the custom antibody preparation are described in the Supplementary Information. The anti-PEG ELISA kit (ab215546) was purchased from Abcam (Cambridge, UK). Bovine serum albumin (BSA), tris buffered saline (TBS), tween-20, streptavidin-alkaline phosphatase (Strep-AP) and p-nitrophenyl phosphate (PNP) tablets were purchased from Sigma Chemical Co (NSW, Australia). All other reagents used were AR grade.

### 2.2. Animals

Male Sprague Dawley rats (260–300 g) were obtained from Monash Animal Services (Monash University, VIC, Australia) and were maintained on a 12 h light/dark cycle at ambient temperature. Rats were provided unlimited access to water, but food was withheld after surgical implantation of cannulas and for 8 h after dosing. All protocols involving animals were approved by the Monash Institute of Pharmaceutical Sciences animal ethics committee.

### 2.3. Preparation of PEGylated Enf

Cysteine-modified Enf was conjugated to PEG-maleimide as previously described by others, with modification [15,16]. N-terminal conjugation was specifically used since C-terminal PEGylation was previously shown to more significantly limit Enf anti-viral activity by Cheng and colleagues [15]. PEG-Maleimide (5 kDa and 20 kDa) was dissolved in 50 mM PBS (pH 7.4) to give concentrations of 20 mg/mL and 50 mg/mL respectively. The conjugation reactions with Cys-Enf were performed via incubation of Cys-Enf (prepared immediately prior to use at a final concentration of 1 mg/mL in PBS) with 2:1 or 5:1 M ratios of 5 kDa PEG or 20 kDa PEG respectively at 4° C overnight. The yield resulting from these reactions was approximately 35–40%. The crude reaction mixtures were then centrifuged at 12,000g prior to separation across a Superdex 75 column (sterile 50 mM PBS mobile phase at a flow rate of 1.5 ml/min) to isolate the mono-PEGylated Peg5-Enf, or Peg20-Enf complex. The eluate was collected in 1 ml fractions and analysed via SDS-PAGE to identify fractions that corresponded to Enf-conjugated PEG. Fractions containing Enf-conjugated PEG were pooled and concentrated using 3 kDa (to isolate Peg5-Enf) or 10 kDa (to isolate Peg20-Enf) MW cutoff Amicon Ultra-15 centrifugal filters. The identity of the final products were confirmed using reducing SDS-PAGE gels with Coomassie staining for protein, followed by barium iodide staining to detect PEG as performed previously [12]. SeeBlue2 was used for the molecular weight markers and approx. 2 µg protein was loaded into each lane. The molecular weight distribution of the final products was characterised by combined size exclusion chromatography-multi-angle light scattering (SEC-MALS) analysis. SEC-MALS was used to identify the molecular weight distribution of the final products from first-principles, as this approach is very accurate for identifying protein molecular weight, and is superior to LC-MS in characterising average molecular weights and polydispersity in complex mixtures, and where protein ionization is poor (particularly with highly PEGylated proteins) [17,18]. Purified PEGylated Enf constructs were then stored in working aliquots at –20 °C and thawed immediately prior to use.

### 2.4. Multi-angle light scattering (SEC-MALS) of PEG-Enf products

SEC-MALS analysis was performed to determine the molecular weight distribution and average molecular weight of PEGylated Enf as

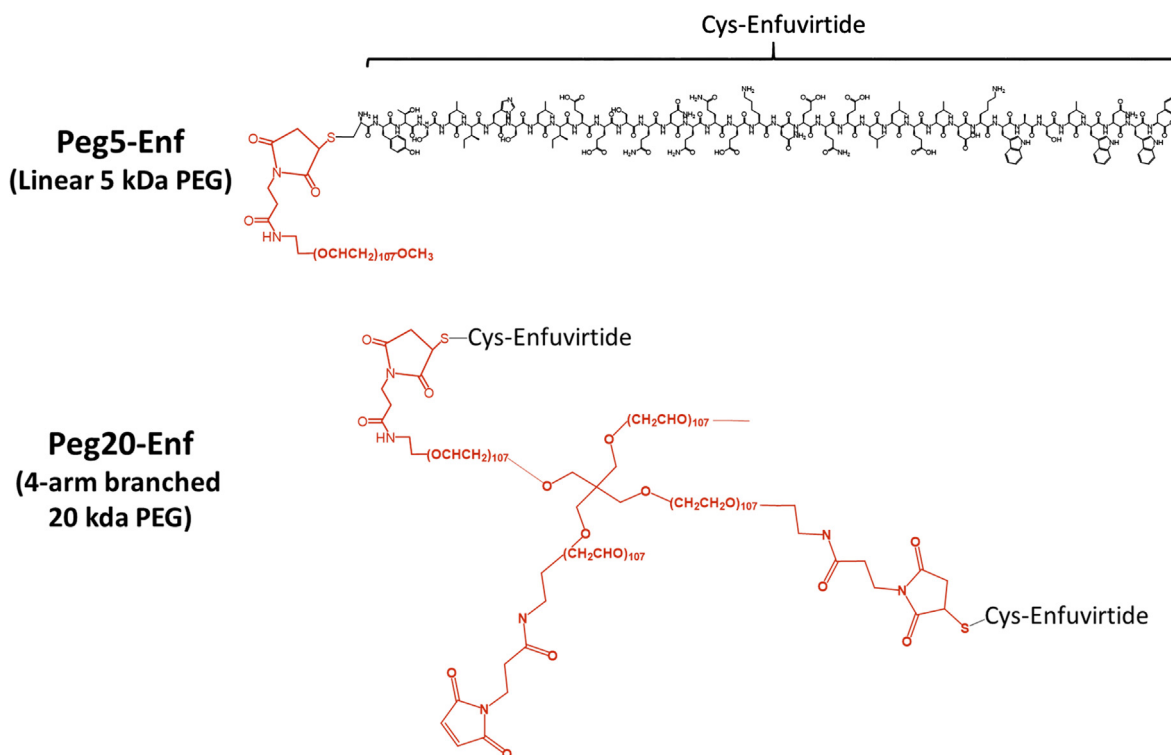


**Fig. 1.** Structure of PEGylated enfuvirtide (Enf) constructs. Peg20-Enf has been represented as the doubly Enf-conjugated PEG product (mixture of *mono*-, *bis*- and *tris*-conjugated Enf) synthesised, rather than the nominal *tris*-Enf conjugated PEG.

previously described [17,19–21]. Peg-Enf (0.15  $\mu\text{g}$  in 50  $\mu\text{l}$ ) was run on a Tosoh TSKgel SuperSW2000 4.6 X 300 mm column equilibrated in PBS at a flow rate of 0.35 ml/min using a Shimadzu LC-20AD isocratic HPLC coupled to a Dawn Heleos MALS detector and an Optilab T-rEX refractive index detector (Wyatt Technologies). Dn/dc values for the PEGylated proteins were measured experimentally under the experimental conditions using the Wyatt refractometer and were 0.174 and 0.163 for the 5 and 20 kDa PEG modified Enf respectively. The molecular weight of the Enf portion of the molecule and the whole PEGylated construct was determined according to the three-detector method [17] using the ASTRA 5 software (Wyatt Technologies).

### 2.5. HIV inhibition assay

The MT-2 cell line [22] and 293T cells were obtained through the NIH AIDS Research and Reference Reagent Program. MT-2 cells were cultured in RF-10 medium (RPMI supplemented with 10% FBS, 100 U/ml penicillin, 100  $\mu\text{g}/\text{ml}$  streptomycin and 2 mM glutamine) as previously described [23]. The 293T cells were cultured in DMEM-10 (supplemented with 10% FBS, 100 U/ml penicillin, 100  $\mu\text{g}/\text{ml}$  streptomycin and 2 mM glutamine) as previously described [24]. All cells were maintained at 37  $^{\circ}\text{C}$  in 5%  $\text{CO}_2$ .

NL4.3, a CXCR4 (X4)-using laboratory strain of human immunodeficiency virus type 1 (HIV-1), was derived by transfection of 293T cells with pDRNL using the calcium phosphate method [24]. Virus supernatant was collected and stored at  $-80^{\circ}\text{C}$  following propagation by infection at least three times in MT-2 cells prior to use in anti-HIV assays.

Assays were performed to determine the anti-HIV activity and cytotoxicity of modified and unmodified Enf in the MT-2T-lymphocyte cell line using cell viability as the measure of virus replication and cytotoxicity as previously described with minor modification [25]. In each assay, viable MT-2 cells were counted using the trypan blue exclusion method and then 50  $\mu\text{l}$  containing  $6.0 \times 10^3$  cells in RF-10 was applied to each well of a 96-well flat-bottomed tissue culture plate

(Nunc, Thermo). Serial 10-fold dilutions of the test compounds and Enf controls were performed in RF-10 medium to  $2 \times$  the final concentrations required. One hundred microliters of the diluted compounds were then added to the MT-2 cells in the 96-well plates in triplicate for both the anti-HIV assay and cytotoxicity assay (including no-compound controls in both assays). For the anti-HIV assay, 100  $\mu\text{l}$  of RF-10 medium was added to create “mock-infected” control wells. All the plates were incubated at 37  $^{\circ}\text{C}$  in 5%  $\text{CO}_2$  for 30 min, followed by the addition of 50  $\mu\text{l}$  of RF-10 containing the 100 TCID<sub>50</sub> (50% Tissue Culture Infective Dose) of HIV NL4.3 to the anti-HIV test wells and 50  $\mu\text{l}$  RF-10 added to the mock-infected and cytotoxicity wells. The assay plates were then incubated for 4–6 days at 37  $^{\circ}\text{C}$  in 5%  $\text{CO}_2$  until complete cell death was observed in the infected, no-compound control wells. At the completion of the assays, cell viability was determined using CellTiter 96 Aqueous One Solution Reagent (Promega) according to manufacturer’s instructions. The 50% effective concentration (EC<sub>50</sub>) and 50% cytotoxicity concentration (CC<sub>50</sub>) values were determined as described [25] by non-linear regression analysis using GraphPad Prism 7.0.

### 2.6. Determination of subcutaneous lymphatic pharmacokinetics in rats

The SC lymphatic pharmacokinetics of unmodified Enf (Fuzeon) and the two PEGylated variants of Enf were evaluated in thoracic lymph duct cannulated rats as previously described [14,26]. Briefly, all rats ( $n = 4$  per group) were cannulated via the right carotid artery to allow serial blood sampling, the right jugular vein to allow replacement of fluid lost via the thoracic lymph duct cannula (via constant infusion of 1.3 ml saline/h) and the thoracic lymph duct (to allow continuous collection of lymph fluid formed posterior to the cannula). All cannulas were then exteriorised through the back of the neck and tunneled through a swivel-tether apparatus to allow blood and lymph sampling from freely moving rats. Rats were allowed to recover overnight in individual metabolism cages prior to dosing.

After overnight recovery from surgery, pre-dose blood samples

(200 µl) were collected from all rats into heparinised (10 IU) eppendorf tubes to provide background correction in ELISAs. Blank lymph was collected overnight into heparinised (200 IU) falcon tubes. Rats were then lightly anaesthetized under isoflurane and administered a dose of 1.2 mg/kg Enf equivalents (of unmodified Enf, Peg5-Enf or Peg20-Enf) SC into the outer right hindleg in a final volume of 0.5 ml/kg saline and then returned to their cages. Enf was administered into this site since it represents the typical clinical injection sites of Enf (Fuzeon; ie. upper arm, thigh, abdomen) and since lymph flows peripherally from this site towards the brachial and axillary lymph nodes prior to draining into systemic circulation above the cannulation point. Using this approach, typical lymphatic concentrations of Enf achieved throughout the body after SC administration can be evaluated. Specifically, absorption of the dose from the SC injection site results in delivery to the blood, followed by redistribution into the lymphatic system as previously described [9]. Serial blood samples (200 µl) were then collected from the carotid artery cannula immediately after dosing and at 0.25, 0.5, 1, 2, 4, 6, 8, 12, 24 and 30 h post dose. Lymph fluid was also collected continuously into heparinised tubes from rats over the time frames 0–1, 1–2, 2–3, 3–4, 4–6, 6–8, 8–12, 12–24, 24–27 and 27–30 h. Plasma was obtained via centrifugation of blood samples at 3500g for 5 min. All plasma and lymph samples as well as standard samples prepared in plasma and lymph on the day of dosing were stored at  $-20^{\circ}\text{C}$  prior to analysis.

Since a terminal elimination phase was not evident in rats delivered Peg20-Enf over 30 h and lymph concentrations were high (suggesting removal of large quantities of Peg20-Enf from systemic circulation via the thoracic lymph duct cannula) a second cohort of rats ( $n = 4$ ) were cannulated only via the carotid artery and dosed SC as above. Serial blood samples were collected in this cohort of rats over 3 days and plasma concentration data from this cohort was used to compare lymph vs plasma concentrations of Peg20-Enf over time, and to compare plasma concentrations across the 3 Enf constructs examined.

### 2.7. Quantification of Enf and Peg-Enf in plasma and lymph samples

Since it is difficult to quantify PEGylated proteins via LCMS-based assay methods, custom monoclonal mouse anti-Enf antibodies were prepared by the Monash Antibody Technologies Facility (Monash University, Vic, Australia) as described in the supplementary information. An anti-Enf ELISA was then developed and validated to quantify Enf in rat plasma and lymph samples, and the protocol and validation for this assay is described in detail in the [supplementary information](#). Acknowledging that the Enf ELISA likely detects some products of Enf catabolism and hydrolysis and that Enf can, in theory, be cleaved from the PEG via hydrolysis near the N-terminus (where the peptide is conjugated to PEG) and subsequently rapidly cleared, a commercial anti-PEG ELISA (ab215546, Abcam) was also used to quantify peptide-modified PEG in plasma and lymph samples in rats dosed with Peg5-Enf or Peg20-Enf according to the manufacturers protocol. In all cases, plasma and lymph samples were quantified against standard curves of the dosed material.

### 2.8. Non-compartmental pharmacokinetic calculations and statistical analyses

All plasma and lymph concentrations were dose-normalised to 1.2 mg/kg Enf equivalents (not based on total construct molecular weight). Terminal (elimination) rate constants ( $k$ ) were determined by regression analysis of individual elimination phases in the plasma concentration – time profiles. The area under the plasma concentration – time curves ( $\text{AUC}_{0-\text{last}}$ ) were calculated using the trapezoid method. The extrapolated area under the plasma concentration-time profiles ( $\text{AUC}_{\text{last}-\infty}$ ) was calculated by dividing the last measured plasma concentration by  $k$ . Plasma elimination half-lives ( $t_{1/2}$ ) were calculated by division of 0.693 by  $k$ . Statistical differences between pharmacokinetic parameters for unmodified Enf and Peg-Enf dosed

animals were evaluated via one-way ANOVA with Tukey's post-test for least significant differences. Significance was determined at a level of  $p < 0.05$ .

### 2.9. Conversion of plasma and lymph exposure in mass units to activity units

Plasma and lymph concentration versus time profiles are reported in terms of both Enf mass per ml (ng/ml as peptide, not of whole PEGylated construct) and Enf mass per ml normalised to anti-viral activity relative to unmodified Enf. Enf concentration normalised to relative activity was calculated by multiplying Enf concentration by (unmodified Enf anti-HIV activity/Peg-Enf anti-HIV activity). The same normalisation calculation was also applied to pharmacokinetic parameters  $C_{\text{max}}$  (maximum concentration in plasma or lymph) and AUC (area under the plasma or lymph concentration versus time profiles) to give a more accurate indication of changes in plasma and lymph exposure to Enf anti-viral activity upon PEGylation.

## 3. Results and discussion

### 3.1. Characterisation of Peg-Enf purity and molecular weight

N-terminal cysteine-modified enfuvirtide (Cys-Enf) was synthesised to allow direct coupling of Enf to PEG-maleimide in high yield and to prevent excessive loss of Enf activity through random conjugation of PEG to primary amine side chains throughout the peptide. In the absence of PEG-maleimide, Cys-Enf largely formed Enf-Enf crosslinks through disulfide formation in the reaction mixture overnight (indicated by the arrow in Fig. 2). In the presence of PEG-maleimide however, formation of the Enf-Enf crosslink was minimal and the yield of PEGylated Enf was high (Fig. 2). Conjugation of 5 kDa linear PEG-maleimide with Cys-Enf yielded the single mono-conjugated Peg5-Enf product in high purity as determined by SDS-PAGE (Fig. 2A & B) and SEC-MALS (9.48 kDa, polydispersity index [PDI] of 1.4; Fig. 2C). Conjugation of the 3 maleimide arm-branched 20 kDa PEG with Cys-Enf, however, yielded a mixture of *mono*-Enf conjugated PEG (25.4 kDa, PDI 1.8 via SEC-MALS), *bis*-Enf conjugated PEG (31 kDa, PDI 2.5 via SEC-MALS) and *tris*-Enf conjugated PEG (41 kDa, PDI 3.6 via SEC-MALS) (Fig. 2A, B, D). Despite significant attempts to optimise the reaction conditions to favour the *tris*-Enf conjugated PEG, the 20 kDa 3-arm branched PEG construct sterically limited formation of this product. Attempts were then made to purify the *bis*-Enf conjugated PEG from *mono*-Enf and *tris*-Enf products via SEC and ion exchange chromatography, but it was not possible to efficiently separate these products in high enough yield to allow biological characterisation. The final product was therefore a mixture of *mono*-Enf, *bis*-Enf and *tris*-Enf PEG conjugates that were present in an approximate molar ratio of 1:1.5:1 as determined by SEC-MALS (Fig. 2D), and showed an average MW of 28.7 kDa and a large polydispersity index of 3.3 resulting from the mixed final product.

### 3.2. Anti-HIV activity of PEGylated and unmodified Enf

The anti-HIV activity of unmodified and modified Enf constructs was examined in the MT-2T-lymphocyte cell line. None of the Enf constructs showed cytotoxic effects up to the maximum concentration of construct applied to the cells (100 µg/ml), consistent with previous observations of others [15]. The EC<sub>50</sub> of the clinical Enf product (Fuzeon) and Cys-Enf was similar (9.6 pmol/ml [0.043 µg/ml] and 10 pmol/ml [0.045 µg/ml] respectively). This value was also similar to previously reported EC<sub>50</sub> values for Enf against the same HIV strain in peripheral blood mononuclear cells (0.016 µg/ml) [16]. Anti-HIV activity was reduced by 3 and over 7-fold for Peg5-Enf and Peg20-Enf respectively (Table 1) as a result of PEGylation (leading to constructs with approximately 50% and 70% w/w PEG loading respectively). This

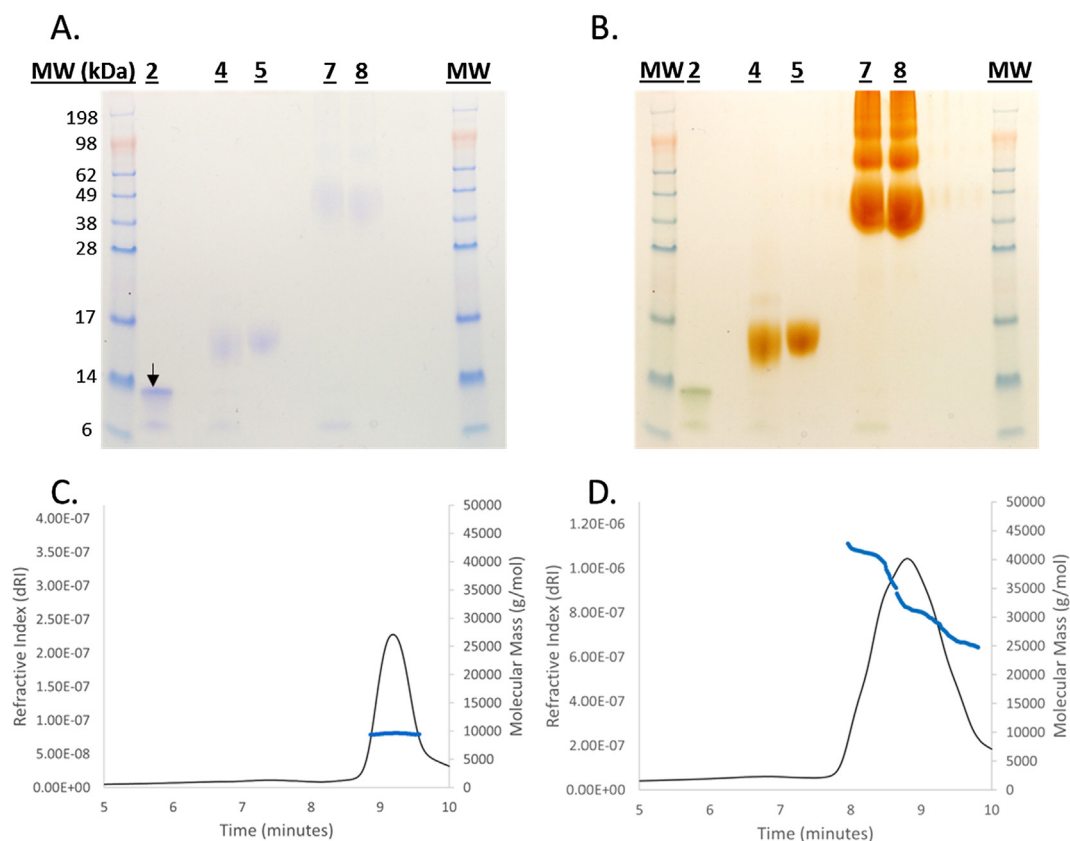


**Fig. 2.** Molecular weight characterisation of PEGylated Enf constructs. Panels A and B: SDS-PAGE gels of Cys-Enf (lane 2), unpurified and purified Peg5-Enf (lane 4 & 5 respectively), unpurified and purified Peg20-Enf (lane 7 & 8 respectively) following coomassie staining for protein (panel A) and I<sub>2</sub>-BaCl<sub>2</sub> staining for PEG (panel B). Arrow indicates crosslinked Cys-Enf formed during overnight reaction in the absence of PEG-maleimide. It should be noted though, that PEGylated proteins run across SDS-PAGE gels at a MW that corresponds to 2 × PEG MW plus the protein MW (ie. giving a band at approx. 15 kDa for the Peg5-Enf material) [27]. Panels C and D: SEC-MALS analysis of Peg5-Enf (Panel C) and Peg20-Enf (Panel D). PEGylated Enf was monitored by normalised differential refractive index and absorbance at 280 nm over time. Molar mass was analysed via MALS by following the total mass by differential refractive index (blue lines) and protein mass by absorbance at 280 nm. (For interpretation of the references to colour in this figure legend, the reader is referred to the web version of this article.)

**Table 1**

Actual and relative anti-HIV activity of unmodified and modified Enf constructs in MT-2 cells. Data represent mean 50% cytotoxic concentration (CC50) and 50% effective concentration (EC50) ± sem (n = 3). Concentrations are reported as pmol of peptide equivalents per ml, not as mass of the whole construct.

Construct	CC <sub>50</sub> (pmol/ml)	EC <sub>50</sub> (pmol/ml)	Enf:Peg-Enf activity ratio
Enf (Fuzeon)	> 20,000	9.6 ± 0.4	–
Cys-Enf	> 20,000	10 ± 1.3	–
Peg5-Enf	> 20,000	28 ± 8	0.34
Peg20-Enf	> 20,000	72 ± 6	0.13

loss of anti-viral activity upon PEGylation is consistent with the results of studies by Huet, who examined the impact of conjugation of Enf to a 2 kDa antithrombin-binding carrier pentasaccharide via PEG linkers of 200–3400 Da [16], and Cheng who examined the anti-viral activity and plasma pharmacokinetics of single 2 kDa PEG and 5 kDa PEG conjugated Enf [15]. The results of the study by Huet showed that the anti-viral activity of 7.1 kDa and 7.8 kDa PEG-linked Enf constructs in human PBMCs varied depending on the HIV strain being examined, with anti-viral activity relative to Enf ranging from unchanged, to a 25 fold reduction. Overall, however, anti-viral activity seemed to be unrelated to the MW of the relatively small conjugated PEGs. This is in contrast to the work by Cheng who showed that conjugation of 2 kDa PEG to Enf resulted in no significant reduction in anti-viral EC50, whilst conjugation of a larger 5 kDa PEG reduced anti-viral activity by approximately 3-fold, consistent with our results. These previous studies

specifically examined the impact of PEGylation with linear PEGs, while the present study considered the use of a 20 kDa branched PEG conjugated to multiple Enf molecules. Although Peg20-Enf was a mixture of *mono*, *bis* and *tris*-Enf conjugates, previous work using 19 kDa interferon showed that while increasing the molecular weight of linear PEGs (thereby increasing PEG loading) led to significant reductions in anti-viral activity, PEG branching had only a minimal (10%) effect on reducing anti-viral activity [14]. In the present study, the reduction in antiviral activity for Peg20-Enf when compared to Peg5-Enf was therefore likely a result of the increased overall PEG loading on the larger construct (~70% w/w PEG compared to ~50% for Peg5-Enf) rather than increased branching.

In other related work, Chang and colleagues reported an improvement in Enf-mediated *in vitro* anti-viral activity by conjugating 4 copies of Enf to several IgG carriers [28]. In this study, several 4-copy Enf-conjugated anti-HIV antibodies were synthesized to examine the ability of these macromolecular complexes to inhibit HIV viral replication in human PBMCs. Each of the Enf-IgG conjugates exhibited 10–100 fold lower EC50 values compared to molar equivalents of Enf alone. This was shown, however, to not be a result of the cell transmission-blocking effects of the antibodies, since conjugation of 4 Enf molecules to a non-HIV active control IgG also improved *in vitro* potency.

### 3.3. Subcutaneous lymphatic pharmacokinetics of PEGylated and unmodified Enf

Previous work has shown that the conjugation of Enf with low MW

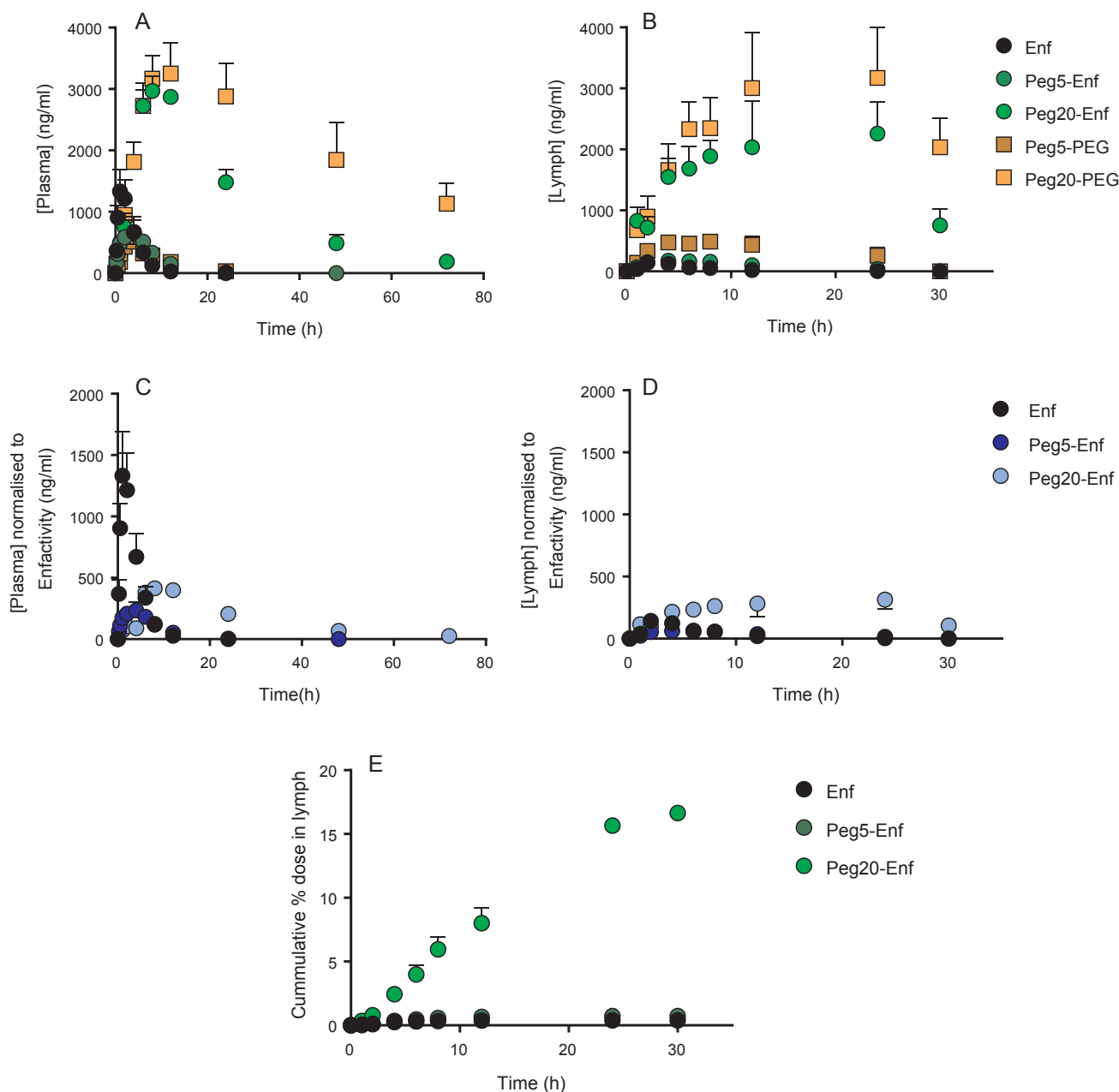


**Fig. 3.** Concentration versus time profiles of unmodified and PEGylated Enf in plasma and lymph after SC administration of 1.2 mg/kg Enf equivalents to rats. Panels represent (A) plasma concentration vs time profiles of Enf constructs after assaying for Enf (green circles) and PEG (brown squares); (B) lymph concentration vs time profiles of Enf constructs after assaying for Enf (green circles) and PEG (brown squares); (C) plasma concentration vs time profiles of Enf constructs (by assaying for Enf) after normalising concentrations to unmodified Enf activity; (D) lymph concentration vs time profiles of Enf constructs (by assaying for Enf) after normalising concentrations to unmodified Enf activity; (E) cumulative % recovery of the SC doses in thoracic duct lymph over 30 h. Data represents mean  $\pm$  s.e.m. ( $n = 4$ ). (For interpretation of the references to colour in this figure legend, the reader is referred to the web version of this article.)

PEG or PEG-pentasaccharide (2–2.5 kDa) can prolong plasma half-life after IV or SC administration by an order of magnitude and double plasma AUC [15,16]. However, the impact of PEGylation on the lymphatic exposure of Enf or other clinically relevant peptides has not been evaluated. This is important since limited exposure of lymphatic HIV reservoirs can lead to plasma viral rebound and potentially the generation of drug-resistant HIV strains [29]. Further, it is important to consider changes to the plasma and lymphatic exposure of modified Enf constructs in the context of changes to anti-viral activity, since both of these factors will have a major role in dictating relative benefit or loss of therapeutic activity *in vivo*. We therefore examined the plasma and lymphatic exposure of unmodified and PEGylated variants of Enf in terms of both Enf concentration and concentration relative to the loss of

anti-viral activity upon PEGylation after SC administration to rats.

Plasma and lymph concentration versus time profiles are shown in Fig. 3, while pharmacokinetic parameters (plasma half-life,  $C_{max}$ , AUC) are shown in Fig. 4. SC administration of Enf resulted in rapid absorption from the injection site ( $T_{max}$  approx. 1.5 h) and rapid elimination from plasma (half-life approximately 2 h) as shown previously by others in rats [15,16]. Conjugation of a single linear 5 kDa PEG slowed absorption from the SC injection site and also resulted in a lower  $C_{max}$  compared to Enf (Fig. 3A). Half-life, however, was only increased by 2-fold (Fig. 4A). The Peg20-Enf construct also exhibited slower absorption from the injection site compared to Peg5-Enf ( $T_{max}$  approx. 8 h), but a significantly higher  $C_{max}$  compared to Enf and Peg5-Enf (Fig. 3A) and an 8-fold slower plasma half-life compared to

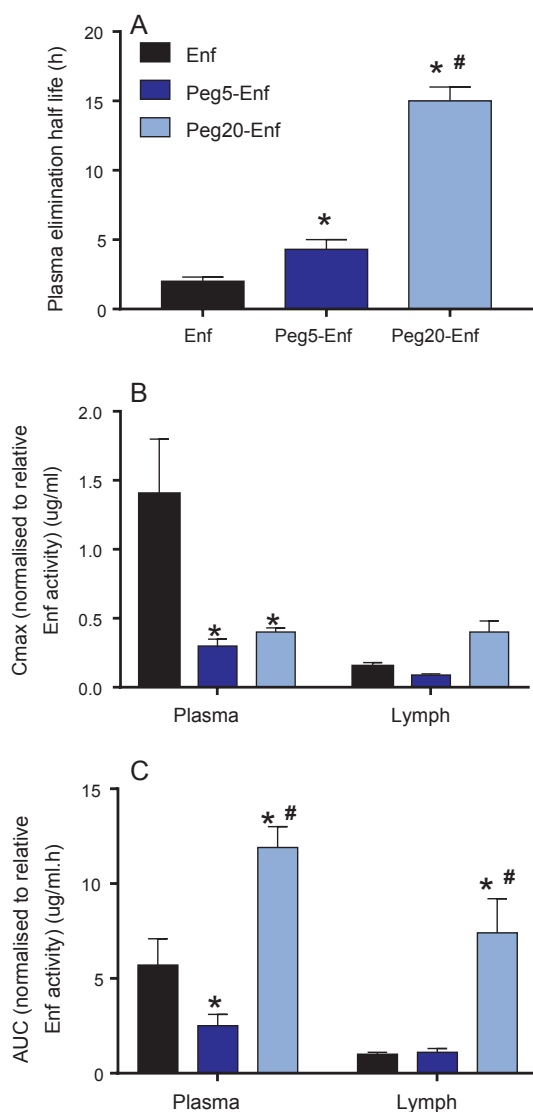


**Fig. 4.** Pharmacokinetic parameters for Enf constructs after SC administration in rats. (A) Terminal elimination half-life in plasma; (B) Cmax in plasma and lymph after normalising concentrations to anti-viral activity relative to unmodified Enf; (C) AUC in plasma and lymph after normalising concentrations to anti-viral activity relative to unmodified Enf. Data represents mean  $\pm$  s.e.m. ( $n = 4$ ). \*Represents  $p < 0.05$  cf. Enf; #Represents  $p < 0.05$  cf. Peg5-Enf.

Enf (Fig. 4A).

We previously examined the impact of PEG molecular weight and branching on the plasma and lymphatic pharmacokinetics of interferon in rats and showed that PEG molecular weight had a more significant impact on dictating plasma pharmacokinetics after SC administration compared to branching [14]. Specifically, a branched 20 kDa PEGylated construct showed a 30% greater AUC compared to a linear 20 kDa construct and identical SC bioavailability. Lymphatic exposure over 30 h however, was unaffected by PEG branching. This suggests that the plasma pharmacokinetics of Peg20-Enf was driven mainly by the high molecular weight PEG which increased the apparent size of the conjugated Enf (thereby reducing renal elimination) and slowed catabolism of the peptide, rather than the branched construction of the PEG.

Examining changes in the plasma pharmacokinetics of Enf after PEGylation alone, however, does not give a clear indication of relative benefit versus detriment of PEGylation to in vivo activity, since PEGylation leads to a loss of intrinsic in vitro protein activity. Plasma concentrations and pharmacokinetic parameters were therefore subjected to a normalisation factor which scaled these concentration-based

parameters to give concentrations relative to anti-viral activity (where relative anti-viral activity of Enf = 1, and anti-viral activity of PEGylated Enf is represented as a fraction of 1 [Table 1]). Normalisation of plasma concentrations to anti-HIV activity relative to Enf therefore revealed that peak activity (Cmax) is reduced upon PEGylation for both PEG constructs (Figs. 3C and 4B), although overall plasma exposure to anti-viral activity (AUC) after a single dose is doubled for Peg20-Enf (Fig. 4C).

The in vivo anti-viral activity of Enf has previously been reported to correlate with minimum (trough) concentrations of Enf during therapy in HIV positive humans, rather than with Cmax or AUC [30]. This suggests that neither the reduction in plasma Cmax, nor the increase in AUC (both relative to Enf activity) for Peg20-Enf is expected to lead to a significant change in in vivo anti-viral activity. However, even after normalising plasma concentrations of Peg20-Enf relative to Enf anti-viral activity, plasma concentrations of Peg20-Enf over 72 h remained within the same concentration range of Enf over 12 h (with plasma concentrations of Enf falling below the assayable limit of quantification by 24 h). This suggests that Peg20-Enf may be expected to provide similar anti-viral activity in plasma to Enf at mass-equivalent doses, but over a longer period of time (3 days relative to 12 h), allowing twice weekly dosing, rather than twice daily dosing.

Lymphatic exposure was also evaluated over 30 h, where thoracic duct lymph was collected continuously after SC dosing. As expected, concentrations of Enf in lymph were low over 12 h after dosing (20–123 ng/ml, Fig. 3B), with Cmax in lymph being an order of magnitude lower than the Cmax in plasma (Fig. 4B). Less than 1% of the entire Enf dose was recovered in thoracic duct lymph over 30 h, further reflecting the very limited lymphatic exposure of Enf after SC administration (Fig. 4E). Interestingly, modification of Enf with 5 kDa PEG did not significantly increase lymphatic exposure as originally hypothesised based on the PEGylated protein literature, and only doubled recovery in thoracic lymph over 30 h. When normalised for activity relative to Enf therefore, lymphatic exposure to Enf activity after SC administration of Peg5-Enf did not differ significantly when compared to unmodified Enf (Fig. 3D, 4B, 4C). In contrast, SC administration of Peg20-Enf led to a significant increase in lymphatic concentrations of Enf (Fig. 3D) and recovery of the SC dose in lymph over 30 h (17%, Fig. 3E). Despite the six-fold lower in vitro anti-viral activity of Peg20-Enf, the notable increase in peak lymphatic concentrations and residence time was sufficient to overcome the loss of activity and led to increases in lymphatic exposure in terms of Enf activity as shown by the two-fold increase in activity-normalised Cmax (though not statistically significant; Fig. 3D, 4B) and a significant five-fold increase in AUC (Fig. 4C). This increase in lymphatic exposure to Enf activity following SC administration of the 29 kDa Peg20-Enf construct (when compared to 4.5 kDa Enf) is believed to result from initial systemic absorption of the peptide (via both the blood and the lymph). This was then followed by extravasation throughout the body and reabsorption in large part via the lymph as a result of the large molecular weight of the construct and high solubility as a result of the PEG, as observed previously with other PEGylated polymers and proteins [9,13]. More recently, this lymphatic redistribution phenomenon has been shown to occur primarily in the liver [31]. As a treatment for HIV however, this may be advantageous since recent work by others has shown that high HIV viral loads significantly increase the risk of liver disease [32]. While the mechanism by which this occurs has not been defined, the investigators proposed that this relationship is linked to the known ability of the HIV virus to activate stellate cells, kill hepatocytes and induce a pro-fibrotic state within the liver, which may also be related to oxidative changes to proteins [33].

Although Enf is not known to be specifically metabolised via peptide cleavage near the N-terminus [34] (where PEG is conjugated), the maleimide-thiol bond may be hydrolysable in vivo to liberate free Enf and Enf metabolites (which would be cleared more rapidly than the intact PEGylated construct) and PEG [35], although to our knowledge this has not been shown before for PEGylated proteins. Furthermore,

apart from a single C-terminal deamidated product that represents the major Enf metabolite (which exhibits a plasma AUC in humans that is 2–15% of the AUC for Enf) Enf is expected to be non-specifically catabolised to its constituent amino acids [36]. Plasma and lymph samples were therefore analysed via ELISA for both Enf (using our custom antibodies) as well as methoxy PEG using a commercial anti-PEG ELISA kit. The results presented in Fig. 3A and B show that interestingly, while plasma and lymph concentrations of Peg5-Enf and Peg20-Enf are similar when assayed for Enf or PEG for the first 4–6 h after dosing, thereafter, the concentration versus time profiles diverge such that concentrations of PEG appear higher than those of Enf. This difference appears to be more significant for the longer circulating Peg20-Enf construct, presumably as a result of the significantly longer exposure time in plasma and lymph when compared to Enf and Peg5-Enf that show relatively similar pharmacokinetics. This suggests that one or both of two clearance mechanisms may be occurring for PEGylated Enf. Firstly, while PEGylation through maleimide-thiol chemistry is a viable approach to prolonging the plasma and lymphatic exposure of peptides and proteins, over time, the PEG may dissociate from the peptide and exhibit absorption, distribution and elimination properties that are independent of the peptide/protein being monitored for pharmacokinetic behavior. Secondly, the Enf ELISA is not specific for intact Enf, and may also detect its major C-terminal deamidated metabolite or a number of catabolism products. However, PEGylation is known to significantly limit protein catabolism in vivo and less than 17% of Enf is deamidated [36], suggesting that the major Enf species detected in plasma and lymph was likely the intact Enf peptide. Further, cleavage of Enf at its three lysine residues abolished detection in the ELISA, suggesting that the assay can only detect a limited range of catabolism products (see supplementary information).

#### 4. Conclusion

In contrast to previous results with PEGylated proteins, PEGylation of the 4.5 kDa peptide enfuvirtide with a low MW PEG failed to significantly improve lymphatic exposure via lymphatic recirculation after SC administration to rats. PEGylation of enfuvirtide with 5 kDa linear PEG slowed absorption from the SC injection site and increased terminal elimination half-life in plasma, but after correcting for the loss of anti-viral activity of the peptide through PEGylation, plasma exposure to anti-viral activity was reduced. In general therefore, it appears that conjugation of enfuvirtide to a 5 kDa PEG to give the approx. 50% PEG-loaded peptide is likely to reduce in vivo anti-viral activity when compared to the administration of enfuvirtide alone at equivalent doses of peptide. In contrast, a 29 kDa enfuvirtide-PEG complex comprised of a branched 20 kDa PEG plus an average of two enfuvirtide peptides improved and prolonged both plasma and lymphatic exposure to the peptide after an equivalent SC dose, despite a six-fold reduction in in vitro anti-viral activity. These results therefore suggest that reformulation of enfuvirtide into an approximately 30 kDa peptide multimer-PEG complex may improve the aqueous solubility of the drug, reduce injection-related pain and improve the in vivo anti-HIV activity of the peptide in both plasma and lymphatic viral reservoirs. Furthermore, this should be achievable with twice weekly SC administration at the same currently utilised dose of peptide compared with existing and painful twice daily injections which are associated with poor compliance.

#### Funding and acknowledgements

This work was supported by a National Health and Medical Research Council project grant. LMK is supported by an NHMRC Career Development fellowship. D.B.A. was supported by a Newton Fund RCUK-CONFAP Grant awarded by The Medical Research Council (MRC) and Fundação de Amparo à Pesquisa do Estado de Minas Gerais (FAPEMIG) (MR/M026302/1, APQ-00828-15), a C.J. Martin Research

Fellowship from the National Health and Medical Research Council of Australia (APP1072476) and the Jack Brockhoff Foundation (JBF 4186, 2016).

#### Conflict of interest

Supplementary information contains the protocol for the preparation of biotinylated and unmodified anti-enfuvirtide antibodies and the developed and validated anti-enfuvirtide ELISA protocol.

#### Appendix A. Supplementary material

Supplementary data to this article can be found online at <https://doi.org/10.1016/j.ejpb.2019.03.008>.

#### References

- [1] Y. Gao, P.F. McKay, J.F.S. Mann, Advances in HIV-1 vaccine development, *Viruses* 10 (2018) E167.
- [2] S. Broder, The development of antiretroviral therapy and its impact on the HIV-1/AIDS pandemic, *Antiviral Res.* 85 (2010) 1–18.
- [3] T.W. Chun, L. Carruth, D. Finzi, X. Shen, J.A. Di Giuseppe, H. Taylor, M. Hermankova, K. Chadwick, J. Margolick, T.C. Quinn, Y.H. Kuo, R. Brookmeyer, M.A. Zeiger, P. Barditch-Crovo, R.F. Siliciano, Quantification of latent tissue reservoirs and total body viral load in HIV-1 infection, *Nature* 387 (1997) 183–188.
- [4] D. Finzi, J. Blankson, J.D. Siliciano, J.B. Margolick, K. Chadwick, T. Pierson, K. Smith, J. Lisiewicz, F. Lori, C. Flexner, T.C. Quinn, R.E. Chaisson, E. Rosenberg, B. Walker, S. Gange, J. Gallant, R.F. Siliciano, Latent infection of CD4+ T cells provides a mechanism for lifelong persistence of HIV-1, even in patients on effective combination therapy, *Nat. Med.* 5 (1999) 512–517.
- [5] C.V. Fletcher, K. Staskus, S.W. Wietgreffe, M. Rothenberger, C. Reilly, J.G. Chipman, G.J. Beilman, A. Khoruts, A. Thorkelson, T.E. Schmidt, J. Anderson, K. Perkey, M. Stevenson, A.S. Perelson, D.C. Douek, A.T. Haase, T.W. Schacker, Persistent HIV-1 replication is associated with lower antiretroviral drug concentrations in lymphatic tissues, *Proc. Natl. Acad. Sci. USA* 111 (2014) 2307–2312.
- [6] M. Harris, P. Patenaude, P. Cooperberg, D. Filipenko, A. Thorne, J. Raboud, S. Rae, P. Dailey, D. Chernoff, J. Todd, B. Conway, J.S. Montaner, Correlation of virus load in plasma and lymph node tissue in human immunodeficiency virus infection. INCAS Study Group. Italy, Netherlands, Canada, Australia, and (United) States, *J. Infect. Dis.* 176 (1997) 1388–1392.
- [7] N.L. Trevasakis, L.M. Kaminskas, C.J. Porter, From sewer to saviour - targeting the lymphatic system to promote drug exposure and activity, *Nat. Rev. Drug Discov.* 14 (2015) 781–803.
- [8] C.J. Porter, S.A. Charman, Lymphatic transport of proteins after subcutaneous administration, *J. Pharm. Sci.* 89 (2000) 297–310.
- [9] L.M. Kaminskas, J. Kota, V.M. McLeod, B.D. Kelly, P. Karellas, C.J. Porter, PEGylation of polylysine dendrimers improves absorption and lymphatic targeting following SC administration in rats, *J. Control. Release* 140 (2009) 108–116.
- [10] A. Supersaxo, W.R. Hein, H. Steffen, Effect of molecular weight on the lymphatic absorption of water-soluble compounds following subcutaneous administration, *Pharm. Res.* 7 (1990) 167–169.
- [11] S.A. Myers, A.A. Selim, M.A. McDaniel, R. Hall, Y. Zhang, J.A. Bartlett, A.L. True, A prospective clinical and pathological examination of injection site reactions with the HIV-1 fusion inhibitor enfuvirtide, *Antivir. Ther.* 11 (2006) 935–939.
- [12] L.J. Chan, D.B. Ascher, R. Yadav, J.B. Bulitta, C.C. Williams, C.J.H. Porter, C.B. Landersdorfer, L.M. Kaminskas, Conjugation of 10 kDa linear PEG onto Trastuzumab Fab' is sufficient to significantly enhance lymphatic exposure while preserving in vitro biological activity, *Mol. Pharm.* 13 (2016) 1229–1241.
- [13] L.M. Kaminskas, D.B. Ascher, V.M. McLeod, M.J. Herold, C.P. Le, E.K. Sloan, C.J. Porter, PEGylation of interferon alpha2 improves lymphatic exposure after subcutaneous and intravenous administration and improves antitumour efficacy against lymphatic breast cancer metastases, *J. Control. Release* 168 (2013) 200–208.
- [14] L.J. Chan, O.M. Feeney, N.J. Leong, V.M. McLeod, C.J.H. Porter, C.C. Williams, L.M. Kaminskas, An evaluation of optimal PEGylation strategies for maximizing the lymphatic exposure and antiviral activity of interferon after subcutaneous administration, *Biomacromolecules* 18 (2017) 2866–2875.
- [15] S. Cheng, Y. Wang, Z. Zhang, X. Lv, G.F. Gao, Y. Shao, L. Ma, X. Li, Enfuvirtide-PEG conjugate: A potent HIV fusion inhibitor with improved pharmacokinetic properties, *Eur. J. Med. Chem.* 121 (2016) 232–237.
- [16] T. Huet, O. Kerbarh, D. Schols, P. Clayette, C. Gauchet, G. Dubreucq, L. Vincent, H. Bompais, R. Mazinghien, O. Querolle, A. Salvador, J. Lemoine, B. Lucidi, J. Balzarini, M. Petitou, Long-lasting enfuvirtide carrier pentasaccharide conjugates with potent anti-human immunodeficiency virus type 1 activity, *Antimicrob. Agents Chemother.* 54 (2010) 134–142.
- [17] L.J. Chan, J.B. Bulitta, D.B. Ascher, J.M. Haynes, V.M. McLeod, C.J. Porter, C.C. Williams, L.M. Kaminskas, PEGylation does not significantly change the initial intravenous or subcutaneous pharmacokinetics or lymphatic exposure of trastuzumab in rats but increases plasma clearance after subcutaneous administration, *Mol. Pharm.* 12 (2015) 794–809.

- [18] M. Chen, Characterising PEGylated proteins by MALS-UV-RI detection, *The Column* 6 (2010) 2–5.
- [19] D.B. Ascher, J. Wielens, T.L. Nero, L. Doughty, C.J. Morton, M.W. Parker, Potent hepatitis C inhibitors bind directly to NS5A and reduce its affinity for RNA, *Sci. Rep.* 4 (2014) 4765.
- [20] C.B. Landersdorfer, S.M. Caliph, D.M. Shackelford, D.B. Ascher, L.M. Kaminskas, PEGylated interferon displays differences in plasma clearance and bioavailability between male and female mice and between female immunocompetent C57Bl/6J and athymic nude mice, *J. Pharm. Sci.* 104 (2015) 1848–1855.
- [21] A. Pacitto, D.B. Ascher, L.H. Wong, B.K. Blaszczyk, R.K. Nookala, N. Zhang, S. Dokudovskaya, T.P. Levine, T.L. Blundell, Lst4, the yeast Fnp1/2 orthologue, is a DENN-family protein, *Open Biol.* 5 (2015) 150174.
- [22] S. Harada, Y. Koyanagi, N. Yamamoto, Infection of HTLV-III/LAV in HTLV-I-carrying cells MT-2 and MT-4 and application in a plaque assay, *Science* 229 (1985) 563–566.
- [23] D. Tyssen, S.A. Henderson, A. Johnson, J. Sterjovski, K. Moore, J. La, M. Zanin, S. Sonza, P. Karellas, M.P. Giannis, G. Krippner, S. Wesselingh, T. McCarthy, P.R. Gorry, P.A. Ramsland, R. Cone, J.R. Paull, G.R. Lewis, G. Tachedjian, Structure activity relationship of dendrimer microbicides with dual action antiviral activity, *PLoS ONE* 5 (2010) e12309.
- [24] S.H. Yap, C.W. Sheen, J. Fahey, M. Zanin, D. Tyssen, V.D. Lima, B. Wynhoven, M. Kuiper, N. Sluis-Cremer, P.R. Harrigan, G. Tachedjian, N348I in the connection domain of HIV-1 reverse transcriptase confers zidovudine and nevirapine resistance, *PLoS Med.* 4 (2007) e335.
- [25] R. Pauwels, J. Balzarini, M. Baba, R. Snoeck, D. Schols, P. Herdewijn, J. Desmyter, E. De Clercq, Rapid and automated tetrazolium-based colorimetric assay for the detection of anti-HIV compounds, *J. Virol. Methods* 20 (1988) 309–321.
- [26] L.M. Kaminskas, V.M. McLeod, D.B. Ascher, G.M. Ryan, S. Jones, J.M. Haynes, N.L. Trevaskis, L.J. Chan, E.K. Sloan, B.A. Finnin, M. Williamson, T. Velkov, E.D. Williams, B.D. Kelly, D.J. Owen, C.J. Porter, Methotrexate-conjugated PEGylated dendrimers show differential patterns of deposition and activity in tumor-burdened lymph nodes after intravenous and subcutaneous administration in rats, *Mol. Pharm.* 12 (2015) 432–443.
- [27] M.M. Kurfurst, Detection and molecular-weight determination of polyethylene glycol-modified hirudin by staining after sodium dodecyl-sulfate polyacrylamide-gel electrophoresis, *Anal. Biochem.* 200 (1992) 244–248.
- [28] C.H. Chang, J. Hinkula, M. Loo, T. Falkeborn, R. Li, T.M. Cardillo, E.A. Rossi, D.M. Goldenberg, B. Wahren, A novel class of anti-HIV agents with multiple copies of enfuvirtide enhances inhibition of viral replication and cellular transmission in vitro, *PLoS ONE* 7 (2012) e41235.
- [29] T.K. Vyas, L. Shah, M.M. Amiji, Nanoparticulate drug carriers for delivery of HIV/AIDS therapy to viral reservoir sites, *Expert Opin. Drug Deliv.* 3 (2006) 613–628.
- [30] M. Thompson, E. DeJesus, G. Richmond, D. Wheeler, J. Flaherty, P. Piliero, A. True, Y.Y. Chiu, Y. Zhang, E. McFalls, G.D. Miralles, I.H. Patel, Pharmacokinetics, pharmacodynamics and safety of once-daily versus twice-daily dosing with enfuvirtide in HIV-infected subjects, *AIDS* 20 (2006) 397–404.
- [31] P. Yadav, V.M. McLeod, C.J. Nowell, L.I. Selby, A.P.R. Johnston, L.M. Kaminskas, N.L. Trevaskis, Distribution of therapeutic proteins into thoracic lymph after intravenous administration is protein size-dependent and primarily occurs within the liver and mesentery, *J. Control. Release* 272 (2018) 17–28.
- [32] H.N. Kim, R. Nance, S. Van Rompaey, J.C. Delaney, H.M. Crane, E.R. Cachay, E. Geng, S.L. Boswell, B. Rodriguez, J.J. Eron, M. Saag, R.D. Moore, M.M. Kitahata, Poorly controlled HIV infection: an independent risk factor for liver fibrosis, *J. Acquir. Immune Defic. Syndr.* 72 (2016) 437–443.
- [33] L.M. Kaminskas, S.M. Pyke, P.C. Burcham, Differences in lysine adduction by acrolein and methyl vinyl ketone: implications for cytotoxicity in cultured hepatocytes, *Chem. Res. Toxicol.* 18 (2005) 1627–1633.
- [34] D. Chang, S.J. Kolis, K.H. Linderholm, T.F. Julian, R. Nachi, A.M. Dzerk, P.P. Lin, J.W. Lee, S.K. Bansal, Bioanalytical method development and validation for a large peptide HIV fusion inhibitor (Enfuvirtide, T-20) and its metabolite in human plasma using LC-MS/MS, *J. Pharm. Biomed. Anal.* 38 (2005) 487–496.
- [35] S.D. Fontaine, R. Reid, L. Robinson, G.W. Ashley, D.V. Santi, Long-term stabilization of maleimide-thiol conjugates, *Bioconjug. Chem.* 26 (2015) 145–152.
- [36] I.H. Patel, X. Zhang, K. Nieforth, M. Salgo, N. Buss, Pharmacokinetics, pharmacodynamics and drug interaction potential of enfuvirtide, *Clin. Pharmacokinet.* 44 (2005) 175–186.